

# On-Chip Integrating Cylinder Cavity for Ultra-Compact NDIR CO<sub>2</sub> Sensors

X. Jia,<sup>1,2\*</sup> J. Roels,<sup>3</sup> R. Baets,<sup>1,2</sup> and G. Roelkens<sup>1,2</sup>

<sup>1</sup> Photonics Research Group, INTEC, Ghent University-imec, Technologiepark 126, 9052 Belgium

<sup>2</sup> Center for Nano- and Biophotonics, Ghent University, Belgium

<sup>3</sup> Melexis Technologies NV, Transportstraat 1, 3980 Tessenderlo, Belgium

*We propose an on-chip integrating cylinder cavity implemented by Deep Reactive Ion Etching(Deep-RIE) of silicon substrates and wafer bonding. The cavity comprises a hollow metallic integrating cylinder with access waveguides. 3D ray-tracing simulation shows that an equivalent optical path length of ~3.5cm can be obtained on a chip area of only 6mm<sup>2</sup>. We performed a CO<sub>2</sub> concentration measurement on the fabricated integrating cylinder, the experiment shows a detection limit of ~100ppm and a response time of less than 3 seconds. The fast sensor response is due to the small footprint of the cavity. The integration of a Mid-IR LED and a photodiode as source and detector is also discussed, showing the potential for a fully integrated miniaturized CO<sub>2</sub> sensor system.*

## Introduction

CO<sub>2</sub> concentration monitoring is essential in numerous applications, such as in smart buildings, greenhouse farming and process control[1]. The existing CO<sub>2</sub> sensors are either based on an electrochemical method or a non-dispersive infrared(NDIR) method. The electrochemical CO<sub>2</sub> sensors measure the change in the electrical properties of materials induced by the CO<sub>2</sub> adsorption, and they have the advantage of being low cost and compact [2,3]. However, electrochemical sensors suffer from short-term stability, low durability and cross-response to other gases (e.g., water vapor) [1]. In NDIR CO<sub>2</sub> sensors, the emission spectrum of the light source is aligned with one of the absorption peaks of CO<sub>2</sub> (typically at 4.25μm), and the CO<sub>2</sub> concentration can be deduced by measuring the absorption of the light by the sample gas. NDIR CO<sub>2</sub> sensors have the advantages of long term stability, high gas specificity and high accuracy[4]. However, in order to achieve high sensitivity, a long interaction length(several cms) is required[5], which makes the sensor bulky and expensive. We propose that by using an on-chip integrating cylinder, the sensor can be miniaturized on a chip area of only ~6mm<sup>2</sup>.

## Fabrication and characterization

Figure 1(a) shows a 3D schematic of the proposed on-chip integrating cylinder, which consists of two silicon substrates. On the bottom substrate, a cylindrical cavity with one input waveguide and two output waveguides is etched by Deep Reactive Ion Etching(Deep-RIE). The top substrate is a planar substrate. A thin layer of gold(~300nm) is sputtered on both substrates to form reflectors. After gold deposition, an Ar plasma treatment (pressure = 53 mTorr, power = 100W, duration = 60s) is applied on both substrates and then the two substrates are bonded using gold-to-gold thermocompression bonding (at 300 °C, 1MPa for 30 minutes).

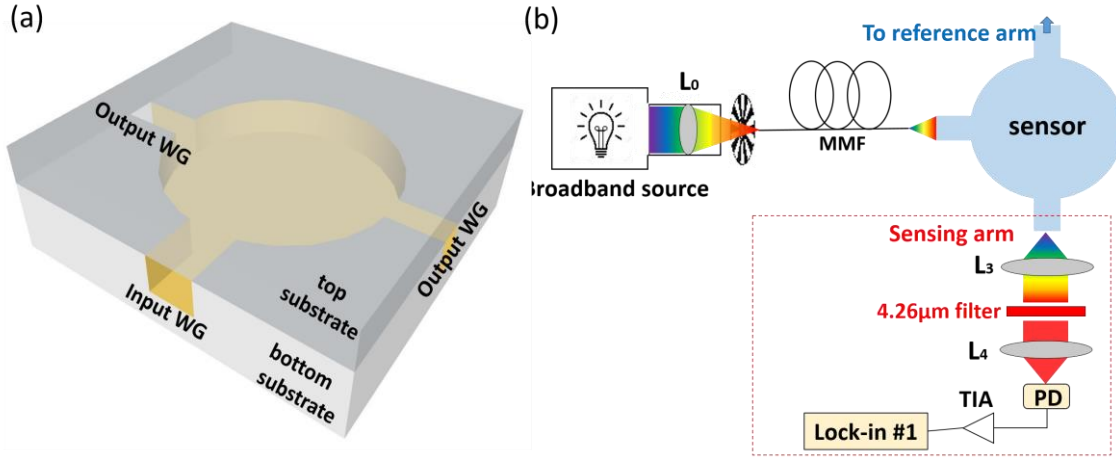


Figure 1: (a) 3D schematic of the integrating cylinder, the diameter and height of the cavity are 4mm and 300 $\mu$ m, respectively, the length and width of the access waveguides are 1mm and 200 $\mu$ m, respectively. (b) Experimental setup. L: lens MMF: multimode fiber, PD: photodiode, TIA: trans-impedance amplifier

To characterize the fabricated integrating cylinder cavity, we built the setup as shown in Figure 1(b). The emitted light from a broadband source is focused by a lens onto a multimode fiber and then is butt-coupled to the input waveguide of the cavity. An optical chopper sits in between the optical source and the multimode fiber to modulate the continuous wave light. Two identical lenses are used to collect the light from the output waveguide and re-focus it onto a photodiode. A bandpass optical filter ( $\lambda = 4.26\mu\text{m}$ , FWHM = 500nm) is sandwiched in between the two lenses. The lens-filter-lens system is sealed and isolated from the ambient. A trans-impedance amplifier (TIA) is designed and fabricated in-house to amplify the signal. At the reference arm, an optical filter with passband centered at  $\lambda = 3.8\mu\text{m}$  (FWHM=500nm) is used, the two arms are otherwise identical. Two lock-in amplifiers (Stanford Research Systems SR830) are used to simultaneously acquire the signals from the sensing and reference arms, and the two lock-in amplifiers are synchronized with identical settings. Sample gas with various  $\text{CO}_2$  concentrations is generated by mixing  $\text{CO}_2$  and  $\text{N}_2$  with two mass flow controllers (MFC), and the sample gas is fed into the cavity by bringing the gas tube in close proximity to the chip.

## **$\text{CO}_2$ sensing results**

Figure 2 shows the normalized absorbance of the integrating cylinder for various  $\text{CO}_2$  concentrations, which is defined by:

$$S = 1 - \frac{I_A}{I_R}$$

Where  $I_A$  and  $I_R$  are signals at sensing and reference arm, respectively. By taking the ratio of the sensing and reference signals, the common mode noise from both arms can be eliminated. It can be seen that as  $\text{CO}_2$  concentration increases, the normalized absorbance also increases, due to the larger absorption by the sample gas. The inset shows the sensor's response to 100ppm  $\text{CO}_2$ , with 10 identical measurements superimposed on top of each other. The response time of the sensor is measured to be  $\sim 2.8\text{s}$  (T90), by purging with 50% of  $\text{CO}_2$  and then abruptly shutting the  $\text{CO}_2$  flow.

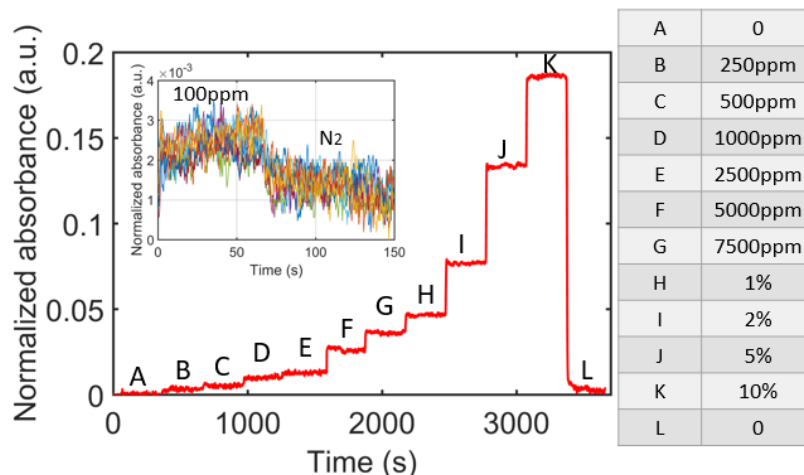


Figure 2: CO<sub>2</sub> sensing result, the concentrations from A to L are listed on the right, the inset shows the response to 100ppm CO<sub>2</sub>, with 10 identical measurements superimposed in one figure.

## LED integration

To integrate the source and detectors on-chip, we propose two structures to couple light from a Mid-IR LED to the input waveguide or from the output waveguide to the photodiode, as shown in Figure 3. In both cases, a trench is etched by using KOH on the planar substrate to house the LED or the photodiode, the inclined mirror in Figure 3(a) can also be fabricated by KOH etching. The coupling efficiency from the LED die to the input waveguide for both structures is simulated by 3D ray-tracing with Zemax, giving 32% and 8%, respectively. The same structures can be used to couple light from the output waveguide to the photodiode, simply by replacing the LED with a photodiode, 3D ray-tracing simulation gives a coupling efficiency of 68% and 43%, respectively.

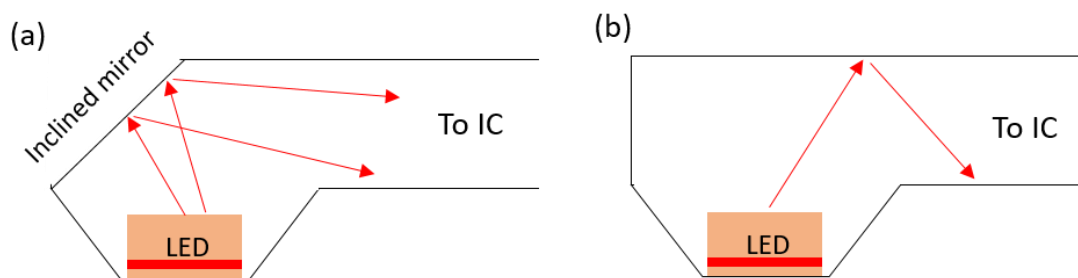


Figure 3: Coupling schemes from the LED die to the input waveguide, or from the output waveguide to the photodiode. The LED die has a dimension of  $L * W * H = 400 \mu\text{m} * 400 \mu\text{m} * 200 \mu\text{m}$ , and the absorption coefficient of the substrate is set to be  $20 \text{ cm}^{-1}$ , the photodiode used for simulation has the same dimensions as the LED.

Figure 4(a) shows a microscope image of the integrated LED on the planar substrate. First, a trench is etched by KOH etching of silicon, after which a contact pad is formed by patterning, gold deposition and lift-off. Then the LED die is flip-chip bonded in the trench (substrate at 350 °C, LED die at 200 °C, pressure = 33MPa, duration = 15 minutes). After bonding, a golden wire bond is applied to connect the top contact of the LED and the contact pad. The integration of the photodiode can be achieved in the same manner.

## Proposed full sensor design

We propose the full sensor design as shown in Figure 4(b). The sensor is formed by wafer bonding of a planar substrate and a Deep-RIE etched substrates. On the planar substrate, a Mid-IR LED and photodiode are integrated in a KOH-etched trench by flip-chip bonding, as shown in Figure 4(a). On the Deep-RIE etched substrate, an integrating cylinder cavity is formed by Deep-RIE. A gas access port is also etched to allow the sample gas to diffuse into the cavity. The full system integration is ongoing and will be characterized at a later stage.

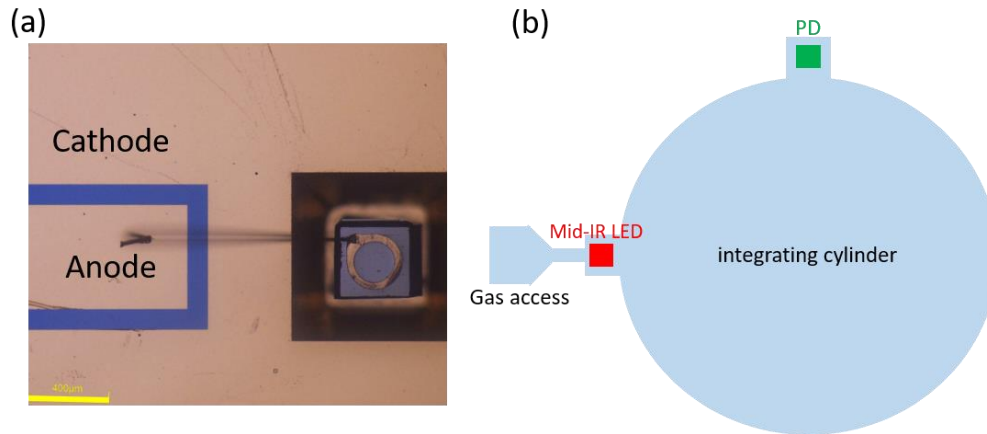


Figure 4: (a) Microscope image of the integrated LED on the top substrate, the LED die has a planar bottom contact and a ring top contact, the trench is 450 μm by 450 μm at the bottom, and the height of the trench is 250 μm, the thickness of the wire bond is 80 μm. (b) Proposed full sensor design, consisting of a Mid-IR LED, a photodiode, and an integrating cylinder.

## Conclusions

In summary, we have demonstrated an integrating cylinder cavity implemented on a silicon chip. CO<sub>2</sub> sensing experiment of the integrating cylinder shows a detection limit of ~100ppm and a response time of ~2.8s, using an external optical source and un-cooled photodiodes. The integration of Mid-IR LEDs and photodiodes is also discussed, as well as our vision for a fully integrated CO<sub>2</sub> sensor system. After integration, the on-chip CO<sub>2</sub> sensor will have a footprint of only 6mm<sup>2</sup>.

## References

- [1] J. Hodgkinson, R.P. Tatam, "Optical gas sensing: a review," *Measurement Science and Technology*, vol. 24(1), 012004, 2012.
- [2] C. Willa, A. Schmid, D. Briand, J. Yuan, and D. Koziej, "Lightweight, Room-Temperature CO<sub>2</sub> Gas Sensor Based on Rare-Earth Metal-Free Composites—An Impedance Study," *ACS Applied Materials & Interfaces*, vol. 9, no. 30, pp. 25553–25558, 2017.
- [3] P. Puligundla, J. Jung, and S. Ko, "Carbon dioxide sensors for intelligent food packaging applications," *Food Control*, vol. 25, no. 1, pp. 328–333, 2012.
- [4] S. Neethirajan, D. S. Jayas, and S. Sadistap, "Carbon Dioxide (CO<sub>2</sub>) Sensors for the Agri-food Industry—A Review," *Food and Bioprocess Technology*, vol. 2, no. 2, pp. 115–121, May 2008.
- [5] K. Thurmond, Z. Loparo, W. Partridge, and S. S. Vasu, "A Light-Emitting Diode- (LED-) Based Absorption Sensor for Simultaneous Detection of Carbon Monoxide and Carbon Dioxide," *Applied Spectroscopy*, vol. 70, no. 6, pp. 962–971, 2016.